Diagnosing Kenya Rainfall in Boreal Autumn: Further Exploration

CHARLES MUTAI

Kenya Meteorological Department, Nairobi, Kenya

DIERK POLZIN AND STEFAN HASTENRATH

Department of Atmospheric and Oceanic Sciences, University of Wisconsin—Madison, Madison, Wisconsin

(Manuscript received 1 August 2011, in final form 28 November 2011)

ABSTRACT

A powerful zonal vertical circulation cell along the Indian Ocean equator controls the boreal autumn rains in Kenya, with a tight negative correlation between surface westerlies (UEQ) and rainfall. UEQ is favored by a steep eastward pressure gradient (PWE) and slow winds in the downstream portion of the South Indian Ocean trade winds (SIW). The high phase of the Southern Oscillation (SO) favors weak SIW, lower pressure in the east, and thus steeper PWE, but that is also affected by pressure in the west. In 1958–97 circulation causalities were most distinct in the regime of abundant rain and slow UEQ, with the SO in the low phase. In the regime of deficient rain and fast UEQ, relationships were less distinct, although the SO was in the high phase almost throughout. In the decade 2001–10, UEQ had a weaker (stronger) correlation with PWE (SIW), the SO was more active and contributing in the proper sense to pressure in the east, but PWE was mainly controlled by pressure in the west. UEQ strongly controlled the rainfall in 1958–97 and 2001–10.

1. Introduction

Over recent years equatorial East Africa experienced alternations of extreme drought and floods. In earlier communications in this journal, we called attention to some events and presented a diagnostic analysis of the circulation mechanisms of Kenya rainfall anomalies (Hastenrath et al. 2007, 2010, 2011). The present article offers an update and a synopsis of events in the first decade of the new century. Evidence is compacted in essential rainfall and circulation indices. Extensive literature references are contained in our previous article (Hastenrath et al. 2011), so they are kept to a minimum here. Section 2 describes the data sources; section 3 presents the essential background; section 4 extends the diagnostics of the 1958–97 era; section 5 explores the events of 2001–10; and a brief synopsis is offered in the closing, section 6.

Corresponding author address: Stefan Hastenrath, Department of Atmospheric and Oceanic Sciences, University of Wisconsin—Madison, 1225 West Dayton Street, Madison, WI 53706.
E-mail: slhasten@wisc.edu

DOI: 10.1175/JCLI-D-11-00414.1

2. Data

As in our previous reports in this journal (Hastenrath et al. 2007, 2010, 2011), the data sources for the present study consist of rain gauge measurements and data archives of circulation information.

Indices of October–November rainfall were compiled for groups of stations indicated in Fig. 1. For the periods 1948–87 and 2001–10, we have indices of all-station averages for the interior highlands (INT) and the coast (CST). The index INT is based on the five highland stations of Nanyuki (NK), Nyeri (NY), Meru (MR), Embu (EM), and Machakos (MK); the index CST is based on the four coastal stations of Lamu (LM), Malindi (MD), Mombasa (MB), and Voi (VO). In addition, we have from earlier work (Hastenrath and Polzin 2003, 2004) the index RON of October–November rainfall compiled over the period 1958–97 from seven coastal stations, including Tanga (TG), Bagamoyo (BA), and Dar es Salaam (DS), as ''all-station average normalized departure,'' using the procedure first introduced by Hastenrath (1976).

The essential data archives of large-scale circulation during 1958–97 and 2001–10 are the Comprehensive Ocean–Atmosphere Data Set (COADS; Woodruff et al.

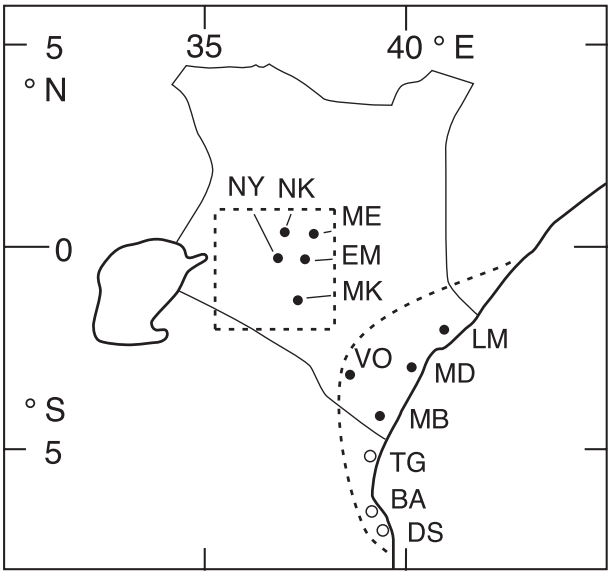

FIG. 1. Orientation map of Kenya, showing domains of rain gauge stations. Five stations—NK, NY, MR, EM, and MK—are used for index INT, and four stations—LM, MD, MB, and VO—for the index CST; additional stations used are for the index RON: TG, BA, and DS.

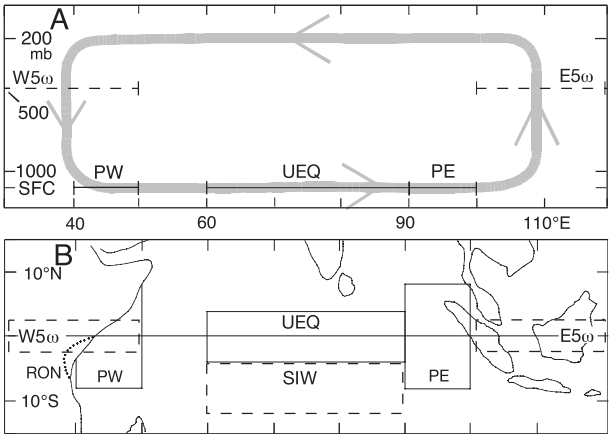

FIG. 2. (a) Zonal vertical cross section and (b) orientation map detailing October–November circulation indices. In (b) solid lines delineate the domains of the indices of UEQ (4°N–4°S, 60°–90°E), of pressure PW (8°N–8°S, 40°–50°E) and PE (8°N–8°S, 90°–100°E), total wind speed in the downstream portion of the South Indian Ocean tradewinds SIW (4–12°S, 60°–90°E), W5ω (2.5°N–2.5°S, 30°–50°E) and E5ω (2.5°N–2.5°S, 100°–120°E), and RON.

1987, 1993) and the National Centers for Environmental Prediction–National Center for Atmospheric Research (NCEP–NCAR) reanalysis (Kalnay et al. 1996; Kistler et al. 2001). The latitude–longitude resolution in COADS is 2° and in NCEP–NCAR it is 2.5°. As for earlier work (Hastenrath et al. 2007, 2010, 2011), various index series for October–November were compiled from these data as detailed in Fig. 2. UEQ (4°N–4°S, 60°–90°E) is an index of the zonal component of the surface wind over the central equatorial Indian Ocean. SIW (4°N–12°S, 60°–90°E) is an index of the total wind speed in the downstream portion of the south Indian Ocean trade winds. PW (8°N–8°S, 40°–50°E) and PE (8°N–8°S, 90°–100°E) are indices of surface pressure in the west and east, respectively, and PWE = PW − PE represents the zonal pressure gradient along the equator. W5ω (2.5°N–2.5°S, 30°–50°E) and E5ω (2.5°N–2.5°S, 100°–120°E) are indices of the 500-mb omega vertical motion. SOI is the Southern Oscillation (SO) index, obtained from online (at http://reg.bom.gov.au/climate/current/soihtm1.shtml).

3. Background

Equatorial East Africa has two rainy seasons centered on April–May and October–November; boreal autumn has the greater spatially coherent variability and has brought severe floods and droughts. Based on the extensive documentation referenced in our earlier reports (Hastenrath et al. 2007, 2010, 2011), the present brief synopsis focuses on the October–November core of the boreal autumn rainy season in East Africa, called ''mvua za vuli,'' referred to as ''vuli.'' An equatorial zonal circulation cell (Fig. 2) features ascending motion (E5ω) over Indonesia, divergent westward flow in the upper troposphere, and subsidence (W5ω) over the western Indian Ocean and East Africa (Hastenrath 2007). This feeds into the surface westerlies (UEQ), which are forced by the strong zonal pressure gradient (PWE), with higher west PW and lower east PE. The westerly surface winds drive the eastward equatorial jet, or Wyrtki jet, in the upper ocean (Wyrtki 1973).

Turning to the interannual variability, the chain of causalities in the coupled ocean–atmosphere system merits attention (Mutai et al. 1998; Mutai and Ward 2000; Hastenrath and Polzin 2004, 2005). The surface equatorial westerlies UEQ form the backbone of the system. Plausibly, UEQ is strong with a steep eastward pressure gradient along the equator and a large PWE; the PWE depends on both the pressure in the west PW and in the east PE. The UEQ is further favored by weak wind speed in the downstream portion of the South Indian Ocean tradewinds SIW, which favors the recurvature of flow (Hastenrath and Polzin 2004). Not detailed here are associations with sea surface temperature (SST), for which extensive literature review is contained in our earlier report (Hastenrath et al. 2011). The wind exerts forcing on the SST field, which can affect the pressure field by hydrostatic forcing.

Table 1 and Fig. 3 highlight the essentials. For the period 1958–97, the rainfall index RON was available. Over

TABLE 1. Matrix of correlation coefficients in hundredths, for October–November. Refer to Figs. 1, 2 for circulation and rainfall indices. (a) Period 1958–97, with asterisks highlighting numbers also plotted in Fig. 3. (b) Period 2001–10. The 5% significance level is 31 for (a) and 63 for (b).

(a) 1958–97

	RON	UEQ	PW	PE	PWE	SIW	W5ω	E5ω
UEQ	−85*							
PW	−52	+52						
PE	+48	−61	−00					
PWE	−70	+86*	+67	−74				
SIW	+69	−68*	−14	+48	−41			
W5ω	−60*	+63*	+20	−43	+45	−30		
E5ω	+46	−74*	−56	+23	−55	+33	−48	
SOI	−56*	+58*	+22	−66	+56	−48	+51	−39

(b) 2001–10

	CST	INT	UEQ	PW	PE	PWE	SIW	W5ω	E5ω
INT	+70								
UEQ	−83	−85							
PW	−05	−31	+19						
PE	+60	+39	−48	+26					
PWE	−69	−54	+71	+59	−33				
SIW	+76	+70	−89	−10	+28	−61			
W5ω	−85	−76	+91	+11	−32	+63	−92		
E5ω	+84	+85	−84	+03	+56	−41	+70	−63	
SOI	−85	−60	+65	−00	−92	+46	−41	+53	−79

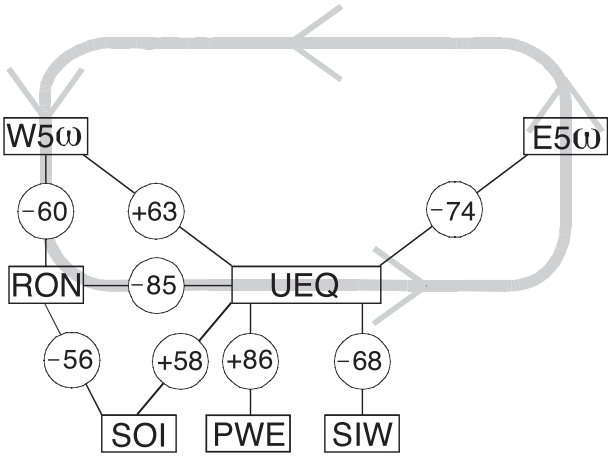

FIG. 3. Diagram of 1958–97 correlations between the circulation indices in Fig. 2 for October–November. Correlation coefficients are in hundredths, and significance is at the 1% level. Shading illustrates schematically the equatorial zonal circulation cell in October–November.

the common interval 1948–87, RON has correlations of +0.94 and +0.80 with the station ensembles at CST and INT, respectively (Fig. 1), with a correlation of +0.70 between these two. RON has an extremely tight correlation with UEQ, which has a strong correlation with PWE and smaller, plausibly positive (negative) correlations with PW (PE) and W5ω (E5ω). Associations with the SOI are plausible: the equatorial westerlies UEQ are forced by the zonal pressure gradient PWE, which in part depends on PE, the pressure in the east, or pressure over the greater Australasian region, which is one of the dipoles of the Southern Oscillation. This appraisal of circulation mechanisms should serve as a basis for the follow-up explorations in the subsequent sections 4 and 5.

4. Vuli of 1958–97

From previous investigations summarized in section 3, we note this inverse chain of causalities: deficient (abundant) boreal autumn rains in equatorial East Africa RON are due to a strong (weak) equatorial zonal circulation cell with enhanced (reduced) subsidence in the west W5ω and eastward moisture transport; a strong (weak) equatorial zonal circulation cell requires fast (slow) UEQ; fast (slow) UEQ is partly due to steep (slack) zonal PWE and partly due to slow (fast) winds in the downstream portion of the South Indian Ocean tradewinds SIW, which are favorable (unfavorable) to the recurvature of the southern trade winds. Pursuing the causality chain further, this leads to some questions. Thus, the zonal pressure gradient PWE is affected by variations of pressure in the west PW and in the east PE, but which is more important? What controls variations in SIW? What are the implications of the SOI? These pending issues shall be examined here from datasets over the four decades of 1958–97.

In part reiterating and mostly complementing the evidence displayed in Fig. 3, Table 1 presents correlations between pertinent indices over the four decades of 1958–97. Most prominent are correlations with RON, UEQ, and PWE. Consistent with these are the correlations of the vertical motions W5ω and E5ω and the pressure in the west PW and east PE. The lack of correlation between PW and PE again confirms the absence of the dipole/seesaw noted in earlier work (Hastenrath and Polzin 2003, 2004). The SIW has large correlations with UEQ and also RON. For the SOI the largest correlation is with PE. Attention in the following is focused primarily on PW, PE, SIW, and SOI in relation to RON and UEQ. With ranking of the 1958–97 series, we identified 10-yr ensembles of contrastingly extreme anomalies in RON and in UEQ.

For RON wet and UEQ slow, the ensembles are overall identical (1961, 1963, 1967, 1968, 1972, 1977, 1978, 1982, 1994, 1997), although the rankings within the 10 yr are not the same. In this ensemble, the zonal pressure gradient PWE was predominantly controlled by PE in 4 yr, by PW in 3 yr, and equally by both in 3 yr. SIW was enhanced in all but one year (1972) when PWE was

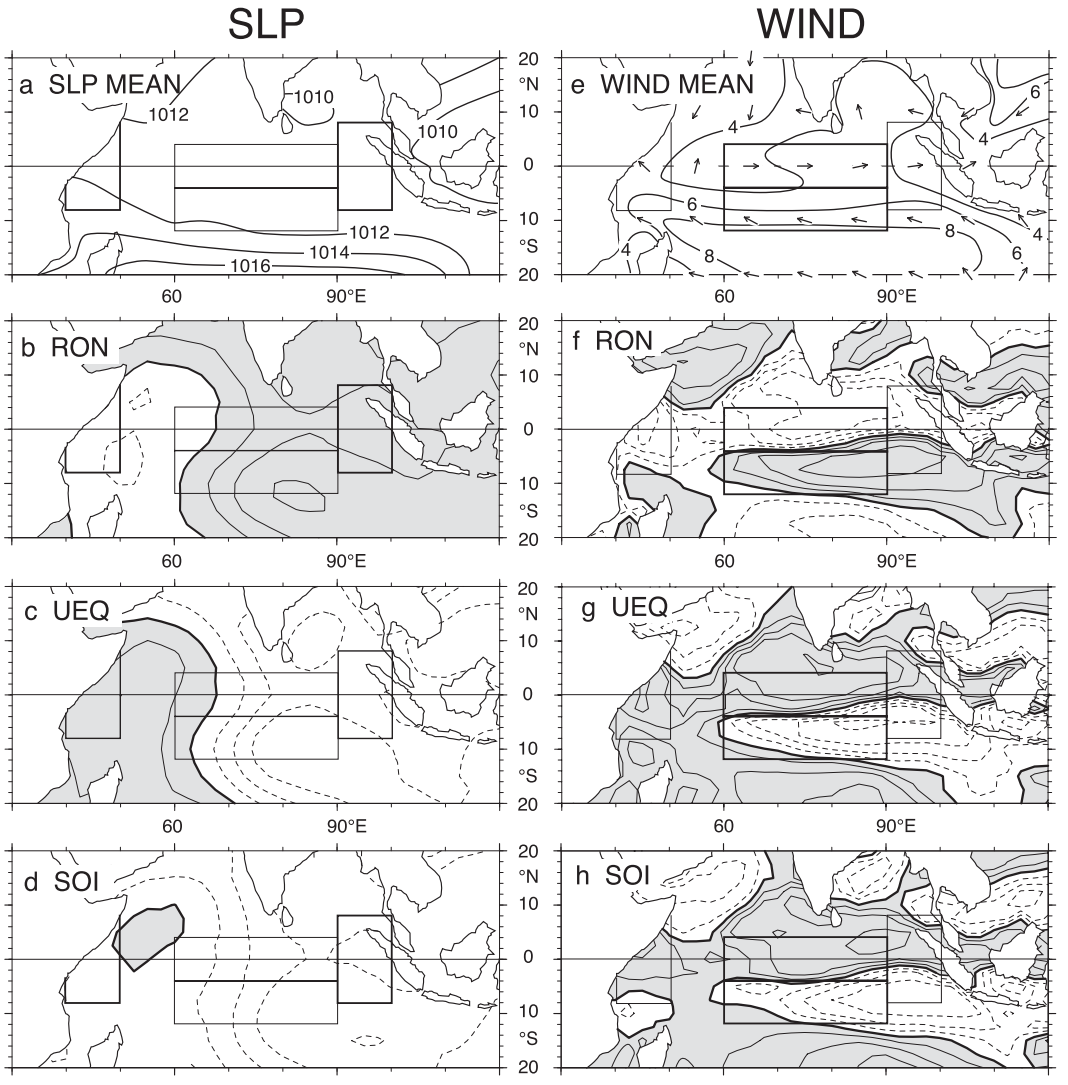

FIG. 4. October–November 1958–97 maps of SLP and wind. As in Fig. 2, rectangles denote the domains of the indices PW, PE, UEQ, and SIW. Mean fields are shown in (a) of SLP with isobar spacing of 2 mb and in (e) of mean resultant wind direction and speed, with isotach spacing of 2 m s^{-1}. Correlations with the SLP field are shown for (b) RON, (c) UEQ, and (d) SOI, and with the total wind speed W for (f) RON, (g) UEQ, and (h) SOI. Isoline spacing is 0.2. The zero line (bold, solid isolines) is shown, as are positive (shading) and negative (dashed lines) values.

particularly slack. The SOI was more negative than the long-term mean in all but one year (1961) when PWE was slack mainly due to reduced pressure in the PW, and SIW was enhanced. Indeed, the year 1961 is a good example: disastrous floods occurred (Thompson and Mörth 1966; Lamb 1966; Flohn 1987; Kapala et al. 1994) when the phase of the SOI was not conducive, just the equatorial westerlies UEQ were extremely weak (Hastenrath and Polzin 2004).

Turning to the opposite extreme ensembles, the ensembles of RON dry (1958, 1959, 1962, 1964, 1970, 1971, 1975, 1979, 1983, 1987) and UEQ fast (1964, 1970, 1973, 1974, 1975, 1983, 1988, 1993, 1995, 1996) have 4 yr in common (1964, 1970, 1975, 1983). In the ensemble of RON dry, the anomalies in the zonal pressure gradient PWE were due to PE in 4 yr, to PW in 4 yr, and to both in 2 yr; SIW was reduced in all but 1 yr (1964) when PWE was particularly steep; the SOI was more positive than the long-term mean in all but 3 yr (1958, 1979, 1987) when PWE was not strong. In the ensemble of UEQ fast, the anomalies in the zonal pressure gradient PWE were due to PE in 7 yr, to PW in 2 yr, and to both in 1 yr (1973). SIW was reduced in 5 yr when PWE was enhanced. The SOI was more positive than the long-term mean in all years.

In synthesis, circulation causalities are most distinct in the regime of RON wet and UEQ slow; the SOI is in

the low phase, high pressure in the east PE contributes to slack zonal pressure gradient PWE, and SIW is enhanced. In the regimes of RON dry and UEQ fast, relationships are less distinct and the regimes are not entirely synchronous, albeit the SOI is positive almost throughout; low pressure in the east PE dominates the steep zonal pressure gradient PWE in the regime of UEQ fast, but not the RON dry; SIW is reduced for RON dry in half of the years and for UEQ fast almost throughout.

Complementing the above appraisal from pertinent circulation indices, Fig. 4 presents maps concerning the October–November 1958–97 pressure and wind fields over the Indian Ocean. Figures 4a,e show the 1958–97 mean fields of sea level pressure (SLP) and wind, respectively. Figures 4b–d show correlation patterns of SLP with RON, UEQ, and the SOI, respectively. Figures 4f–h show the corresponding correlation patterns of the total wind speed with RON, UEQ and the SOI, respectively. Figures 4a,e should serve as a reference and orientation for the appraisal of the correlation maps. From Table 1a, it is recalled that RON and UEQ have an extremely tight negative correlation, and accordingly the patterns are inverse and very similar in Fig. 4b versus Fig. 4c for SLP, and in Fig. 4f versus Fig. 4g for wind. Likewise, the SOI has strong correlations: negative with RON and positive with UEQ. Consistent with that, the patterns are similar but inverse in Fig. 4d versus Fig. 4b and in Fig. 4h versus Fig. 4f. The patterns are similar and of the same sign in Fig. 4d versus Fig. 4c, and Fig. 4h versus Fig. 4g, which are particularly similar.

Figures 4b–d are pertinent with respect to the pressure indices PW and PE, showing the broader context of PW having a negative correlation with RON and the SOI and a positive correlation with UEQ. Particularly noteworthy are the strong negative correlations extending into the central portion of the southern Indian Ocean in Figs. 4c,d, indicating low pressure in the high phase of the SOI. Figures 4f–h are most informative with respect to the wind indices UEQ and SIW. In particular, Figs. 4g,h show a band of strong negative correlations to the south of the equator. These should be appreciated in the context of the pressure correlations in Figs. 4c,d; indeed, lower pressure at 10°–20°S favors weaker wind in the downstream portion of the South Indian Ocean tradewinds SIW, which is conducive to faster UEQ, which is also apparent in Figs. 4g,h. In context, the high phase of the SOI favors strong UEQ through two complementary contributions (Figs. 4d,h): low pressure in the east PE (Figs. 4e,d) and reduced pressure in the central part of the south Indian Ocean, which entails weaker wind in the downstream portion of the South Indian Ocean tradewinds SIW, which favors a recurvature of flow and fast UEQ.

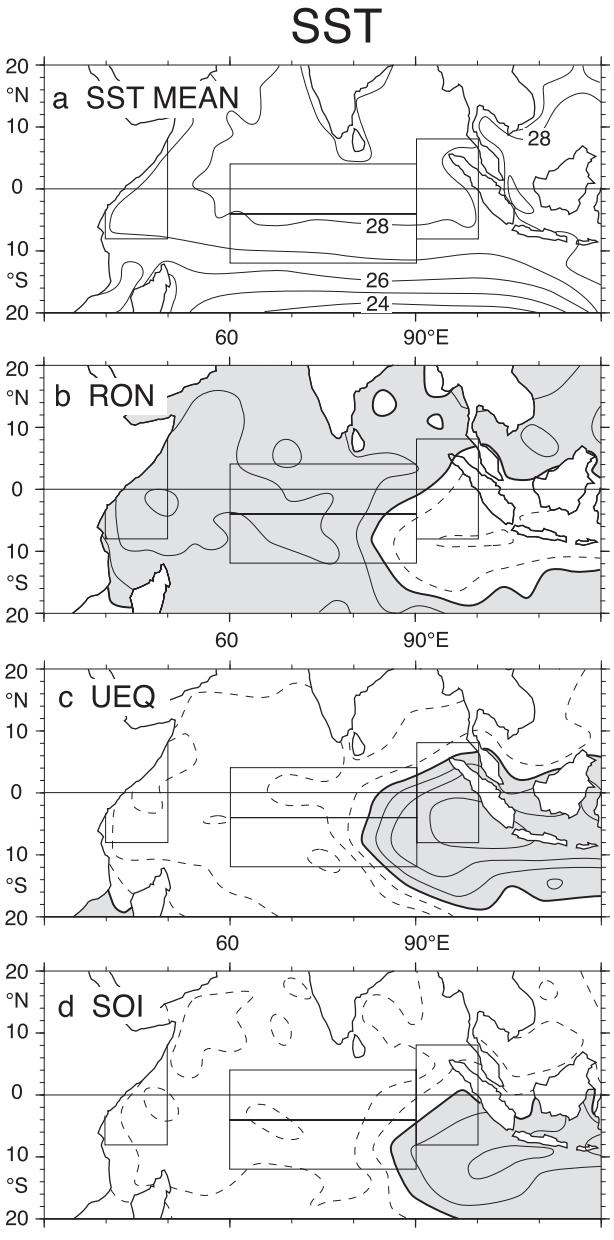

FIG. 5. October–November 1956–97 maps of SST. As in Figs. 2, 4, rectangles denote the domains of the indices PW, PE, UEQ, and SIW. Mean field of SST is shown in (a) with isotherm spacing of 1°C. Correlations with the SST field are shown for (b) RON, (c) UEQ, and (d) SOI. Isoline spacing is 0.2. The zero line (bold, solid isolines) is shown, as are positive (shading) and negative (dashed lines) values.

Figure 5 presents the maps concerning the SST field. The long-term mean map in Fig. 5a features the colder waters in the south versus north and west versus east in the equatorial band. The correlation map in Fig. 5b for RON displays the positive (negative) values in the west (east), consistent with Figs. 4b,f. Repeating earlier work (Hastenrath and Polzin 2004), Fig. 5c for UEQ shows

TABLE 2. Rainfall and circulation indices of October–November 2001–10, as 10-yr mean and departures. Units for CST and INT in mm; for UEQ and SIW in m s^{-1}; for PWE in mb, and for PW and PE in mb above 1000; for W5ω and E5ω in 10^{-4} mb s^{-1}; and SOI is dimensionless.

	CST	INT	UEQ	SIW	PWE	PW	PE	W5ω	E5ω	SOI
Mean	172	329	+3.0	+5.7	+2.2	12.3	10.1	+0.3	−4.8	−2.3
2001	−39	−41	+1.4	−0.6	+2.0	+1.5	−0.5	+0.3	−0.1	+2.7
2002	+46	−20	−1.6	+0.6	+0.2	+0.3	+0.1	−0.7	+1.0	−6.7
2003	−34	+74	+0.3	−0.4	+0.9	−0.4	+0.5	+0.6	+0.5	−2.7
2004	+66	+41	−0.6	−0.3	−0.6	−0.3	+0.3	−0.6	+1.1	−6.5
2005	−64	−88	+1.4	−0.7	+1.0	+1.6	+0.6	+1.5	−0.8	+4.1
2006	+173	+175	−4.1	+2.1	−1.0	+0.4	+0.6	−2.7	+2.0	−8.4
2007	−64	+40	+0.0	−0.1	0.0	−1.1	−1.1	+0.5	−0.5	+7.6
2008	−80	−59	+0.1	−0.1	−0.2	−0.5	−0.3	+0.1	−1.3	+15.3
2009	+84	−16	+0.1	−0.1	−0.8	−0.5	+0.3	+0.2	−0.4	−10.7
2010	−84	−105	+2.9	−0.3	+1.1	+0.2	−0.9	+0.8	−1.4	+17.4

negative (positive) values in the west (east). Figure 5d for the SOI features negative (positive) values in the northwest (southeast). Considering the strong correlation of UEQ with RON and the SOI (Table 1), the patterns in Figs. 5b–d are plausibly consistent with earlier findings (Hastenrath and Polzin 2005, their Fig. 6). Thus, anomalies in the wind field lead those in SST, which in turn can hydrostatically affect the pressure field.

5. Vuli of 2001–10

Building on the diagnostic appraisal of circulation mechanisms in section 4, the present section considers events in the first decade of the new century. The pertinent evidence is presented in Tables 1b, 2. The 10-yr matrix in Table 1b is broadly consistent with the 40-yr matrix in Table 1a. It should be noted that the 5% significance level requires a correlation that is twice as large in Table 1b than in Table 1a. Most remarkable in comparing periods 2001–10 to 1958–97 are the strong correlation of UEQ with CST, INT, and RON; the weaker (stronger) correlation of UEQ with PWE (SIW); the stronger correlation of the SOI with PE and with CST.

Table 2 details the circulation characteristics of the 10 yr of 2001–10. The W5ω had less (more) subsidence in the wet (dry) years and with slow (fast) UEQ: the wet years of 2002, 2004, and 2006 had slow UEQ; the dry years of 2001, 2005, and 2010 had fast UEQ; and it was less extreme in the dry years of 2007 and 2008. The slow UEQ in 2004 and 2006 came with slack PWE and in 2006 with fast SIW; the fast UEQ in 2001, 2005, and 2010 came with steep PWE and slow SIW. The PWE was mainly controlled by PW in 2001, 2002, 2005, 2008, and 2009; mainly by PE in 2006 and 2010; and about equally by both PW and PE in 2003, 2004, and 2007. The SOI contributed in the proper inverse sense to PE in all years except 2005 and to SIW in all years except 2003, 2004, and 2009. Only in the 3 years of 2001, 2003, and 2005 was the SOI smaller than 5 in absolute value, as compared to 21 yr in the course of 1958–97. In perspective, SOI appeared active in this first decade of the new century; it contributed in the proper sense to PE in almost all years, but PWE was mainly controlled by PW. The SOI contributed in the proper sense to SIW, and SIW together with PWE controlled UEQ, which strongly controlled the rainfall (CST and INT) in 2001–10, as it (RON) did in 1958–97.

6. Conclusions

Of the two rainy seasons in equatorial East Africa, the boreal autumn rains (mvua za vuli) centered on October–November merit particular attention. Then surface westerlies sweep the central equatorial Indian Ocean and become the backbone of a powerful zonal vertical circulation cell along the Indian Ocean equator. The boreal autumn rains are extremely tightly correlated with the surface westerlies (UEQ). The development of UEQ is favored by weak wind speed in the downstream portion of the south Indian Ocean trade winds (SIW), and plausibly fast UEQ comes with steep eastward pressure gradient along the equator (PWE), which depends on both pressure in the west (PW) and east (PE). The PE is in the greater Australasian region and is thus associated with the SO.

In 1958–97 circulation causalities were most distinct in the regime of abundant rain and slow UEQ, with the SO in the low phase and increased pressure in the east contributing to slack PWE and enhanced SIW. In the regime of deficient rain and fast UEQ, the relationships were less distinct, albeit the SO was in the high phase almost throughout. The SO is correlated negatively with pressure in the east and SIW, and thus positively with

UEQ. Remarkably, the disastrous flood year 1961 featured slow UEQ with slack PWE dominated by low pressure in the west, while the phase of SO was not conducive.

In the decade of 2001–10 compared to 1958–97, UEQ had a weaker (stronger) correlation with PWE (SIW); the SO was more active and contributing in the proper sense to pressure in the east, but PWE was mainly controlled by pressure in the west. SO contributed in the proper sense to SIW, and SIW together with PWE controlled UEQ, which strongly controlled the rainfall in 2001–10 and 1958–97.

In conclusion, the observational evidence from the twentieth century and the new century shows that the rainfall of vuli is dominated by the equatorial zonal circulation cell, as manifested in the tight association with UEQ; the UEQ is controlled by PWE or PW and PE (which vary without dipole/seesaw) and by SIW; the SO can affect PE and SIW and thus contribute to the chain of causalities affecting UEQ.

Acknowledgments. This study was supported by the Variability of Tropical Climate Fund of the University of Wisconsin Foundation. We appreciate having access to the COADS and NCEP–NCAR reanalysis datasets and the Kenya rainfall data, which made this appraisal of circulation and climate anomalies possible. We thank the reviewers for their feedback.

REFERENCES

Flohn, H., 1987: East African rains of 1961/62 and the abrupt change of the White Nile discharge. *Palaeoecol. Africa,* **18,** 3–18.

Hastenrath, S., 1976: Variations in low-latitude circulation and extreme climatic events in the tropical Americas. *J. Atmos. Sci.,* **33,** 202–215.

——, 2007: Circulation mechanisms of climate anomalies in East Africa and the equatorial Indian Ocean. *Dyn. Atmos. Oceans,* **43,** 25–35.

——, and D. Polzin, 2003: Circulation mechanisms of climate anomalies in the equatorial Indian Ocean. *Meteor. Z.,* **12,** 81–93.

——, and ——, 2004: Dynamics of the surface wind field over the equatorial Indian Ocean. *Quart. J. Roy. Meteor. Soc.,* **130,** 503–517.

——, and ——, 2005: Mechanisms of climate anomalies in the equatorial Indian Ocean. *J. Geophys. Res.,* **110,** D08113, doi:10.1029/2004JD004981.

——, ——, and C. Mutai, 2007: Diagnosing the 2005 drought in equatorial East Africa. *J. Climate,* **20,** 4628–4637.

——, ——, and ——, 2010: Diagnosing the droughts and floods in equatorial East Africa during boreal autumn 2005–08. *J. Climate,* **23,** 813–817.

——, ——, and ——, 2011: Circulation mechanisms of Kenya rainfall anomalies. *J. Climate,* **24,** 304–312.

Kalnay, E., and Coauthors, 1996: The NCEP/NCAR 40-Year Reanalysis Project. *Bull. Amer. Meteor. Soc.,* **77,** 437–471.

Kapala, A., K. Born, and H. Flohn, 1994: Monsoon anomaly or an El Nino event at the equatorial Indian Ocean? Catastrophic rains 1961/62 in East Africa and their teleconnections. *Proceedings of the International Conference on Monsoon Variability and Prediction,* Vol. 1, WCRP-84, WMO/TD 619, World Meteorological Organization, 119–125.

Kistler, R., and Coauthors, 2001: The NCEP–NCAR 50-Year Reanalysis: Monthly means CD-ROM and documentation. *Bull. Amer. Meteor. Soc.,* **82,** 247–267.

Lamb, H. H., 1966: Climate in the 1960's: Changes in the world's wind circulation reflected in prevailing temperatures, rainfall patterns and the levels of the African lakes. *Geogr. J.,* **132,** 183–212.

Mutai, C. C., and M. N. Ward, 2000: East African rainfall and the tropical circulation/convection on intraseasonal to interannual timescales. *J. Climate,* **13,** 3915–3939.

——, ——, and A. W. Colman, 1998: Towards the prediction of the East Africa short rains based on sea-surface temperature–atmosphere coupling. *Int. J. Climatol.,* **18,** 975–997.

Thompson, B. W., and H. Mörth, 1965: Notes from East Africa, No. 1. *Weather,* **20,** 226–227.

Woodruff, S. D., R. J. Slutz, R. L. Jenne, and P. M. Steurer, 1987: A Comprehensive Ocean-Atmosphere Data Set. *Bull. Amer. Meteor. Soc.,* **68,** 1239–1250.

——, S. Lubker, K. Wolter, S. J. Worley, and J. D. Elms, 1993: Comprehensive Ocean-Atmosphere Data Set (COADS) release 1a: 1980-92. *Earth Syst. Monit.,* **4,** 1–8.

Wyrtki, K., 1973: An equatorial jet in the Indian Ocean. *Science,* **181,** 262–264.